SUPPLEMENTARY APPENDIX

A 3D iPSC-differentiation model identifies interleukin-3 as a regulator of early human hematopoietic specification

Mania Ackermann,[1,2] Kathrin Haake,[1,2] Henning Kempf,[2,3,4] Paul Kaschutnig,[5] Anna-Carina Weiss,[6] Ariane H.H. Nguyen,[1,2] Markus Abeln,[7] Sylvia Merkert,[2,3] Mark Phillip Kühnel,[8,9] Dorothee Hartmann,[10] Danny Jonigk,[2,8,9] Thomas Thum,[2,10] Andreas Kispert,[6] Michael D. Milsom[5] and Nico Lachmann[1,2]

[1]Institute of Experimental Hematology, Hannover Medical School, Hannover, Germany; [2]REBIRTH Center for Translational Regenerative Medicine, Hannover Medical School, Hannover, Germany; [3]Leibniz Research Laboratories for Biotechnology and Artificial Organs (LEBAO), Department of Cardiothoracic, Transplantation and Vascular Surgery, Hannover Medical School, Hannover, Germany; [4]Department of Stem Cell Discovery, Novo Nordisk A/S, Maaloev, Denmark; [5]German Cancer Research Center (DKFZ), Division of Experimental Hematology and Heidelberg Institute for Stem Cell Technology (HI-STEM), Heidelberg, Germany; [6]Institute of Molecular Biology, Hannover Medical School, Hannover, Germany; [7]Institute of Clinical Biochemistry, Hannover Medical School, Hannover, Germany; [8]Institute for Pathology, Hannover Medical School, Hannover, Germany; [9]Biomedical Research in Endstage and Obstructive Lung Disease (BREATH), German Center for Lung Research, Hannover, Germany and [10]Institute of Molecular and Translational Therapeutic Strategies (IMTTS), Hannover Medical School, Hannover, Germany

 doi:10.3324/haematol.2019.228064

Received: May 28, 2019.

Accepted: March 25, 2020.

Pre-published: April 23, 2020.

Correspondence: *NICO LACHMANN* - lachmann.nico@mh-hannover.de

Supplementary Information

A 3D iPSC-differentiation model identifies interleukin-3 as a regulator of early human hematopoietic specification

Mania Ackermann[1,2], Kathrin Haake[1,2], Henning Kempf[2,3,4], Paul Kaschutnig[5], Anna-Carina Weiss[6], Ariane HH Nguyen[1,2], Markus Abeln[7], Sylvia Merkert[2,3], Mark Phillip Kühnel[8,9], Dorothee Hartmann[10], Danny Jonigk[2,8,9], Thomas Thum[2,10], Andreas Kispert[6], Michael D Milsom[5], Nico Lachmann[1,2,#]

Supplementary Figures:

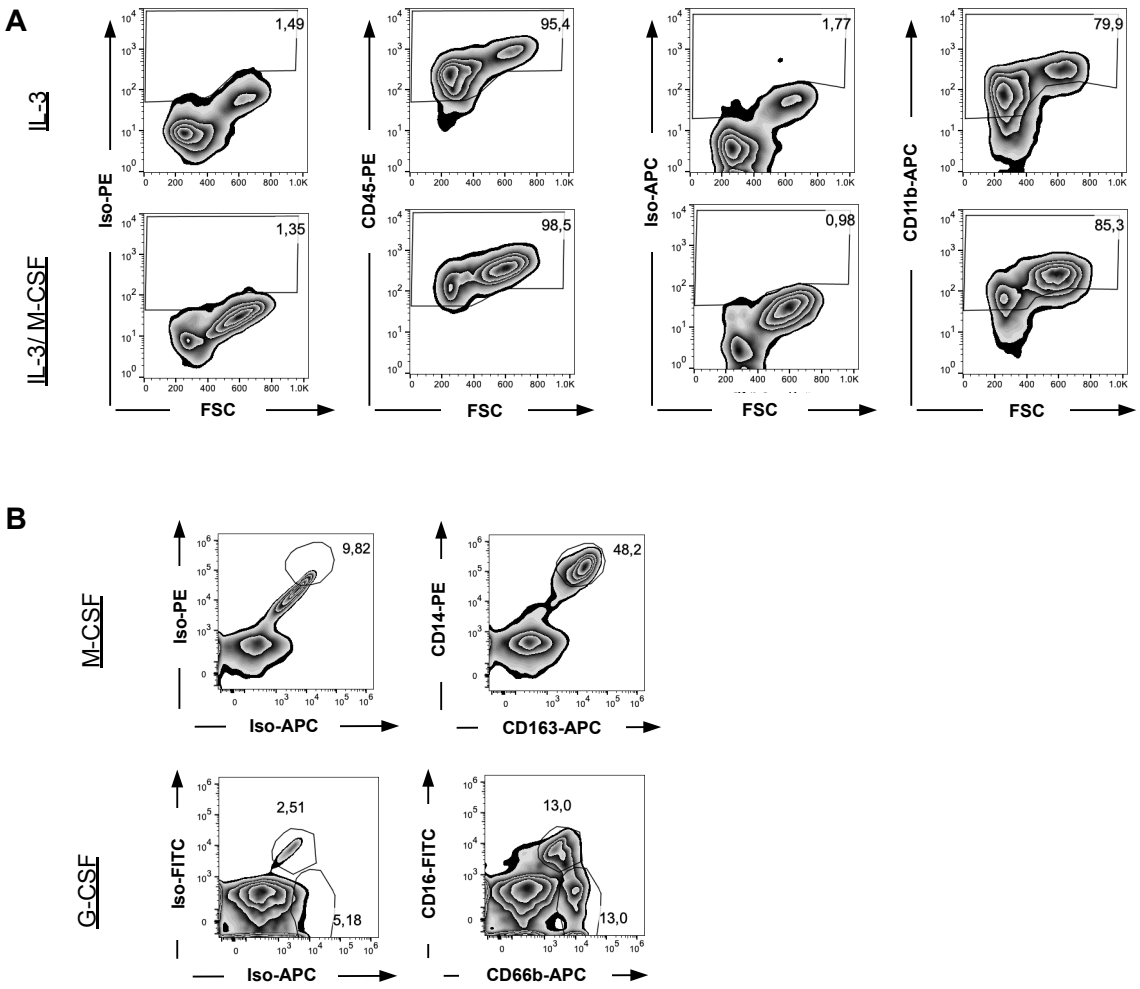

Supplementary Figure 1. Effect of IL-3 on hematopoietic differentiation of human iPSC. (A) Flow cytometry analysis of CD45 and CD11b surface expression on cells harvested from the supernatant of differentiation cultures with only IL-3 and IL-3/ M-CSF (percentage of gated population is indicated). **(B)** Flow cytometry analysis of cells harvested from cultures with only IL-3 that were further matured for 1 week in medium with M-CSF (upper row) or G-CSF (lower row, percentage of gated population is indicated).

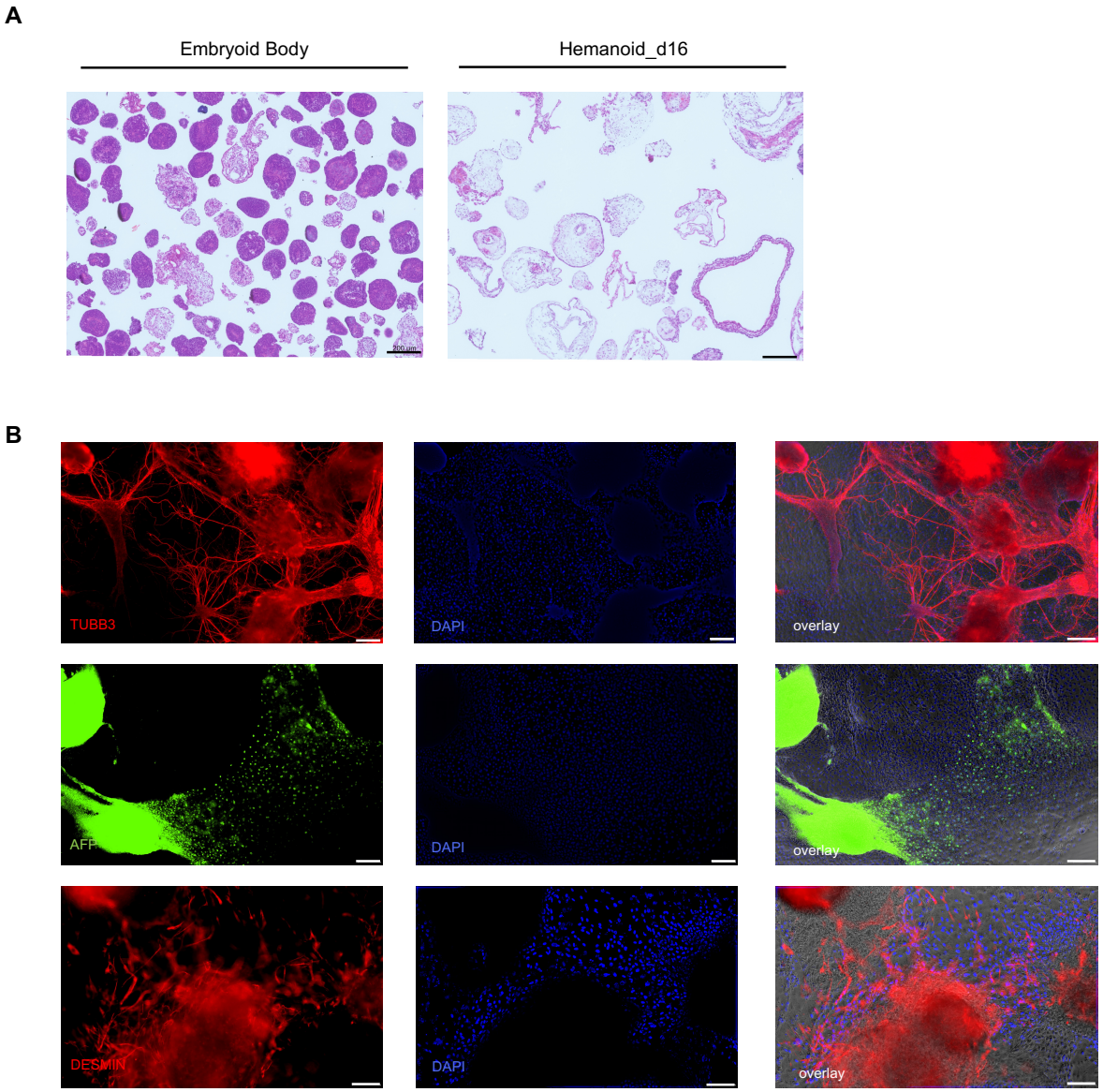

Supplementary Figure 2. Characterization of hemanoids by analysis of paraffin sections and immunofluorescent staining. (A) Hematoxilin/Eosin staining of paraffin sections derived from embryoid bodies (left) and hemanoids_d16 (right). **(B)** Hemanoids were fixed with PFA and subjected to immunofluorescent staining for TUBB3 (Tubulin) (upper row), FOXA2 (middle) and DESMIN (lower row) at day 16 of differentiation (scale bar 200μm for TUBB3 and AFP, 100μm for DESMIN).

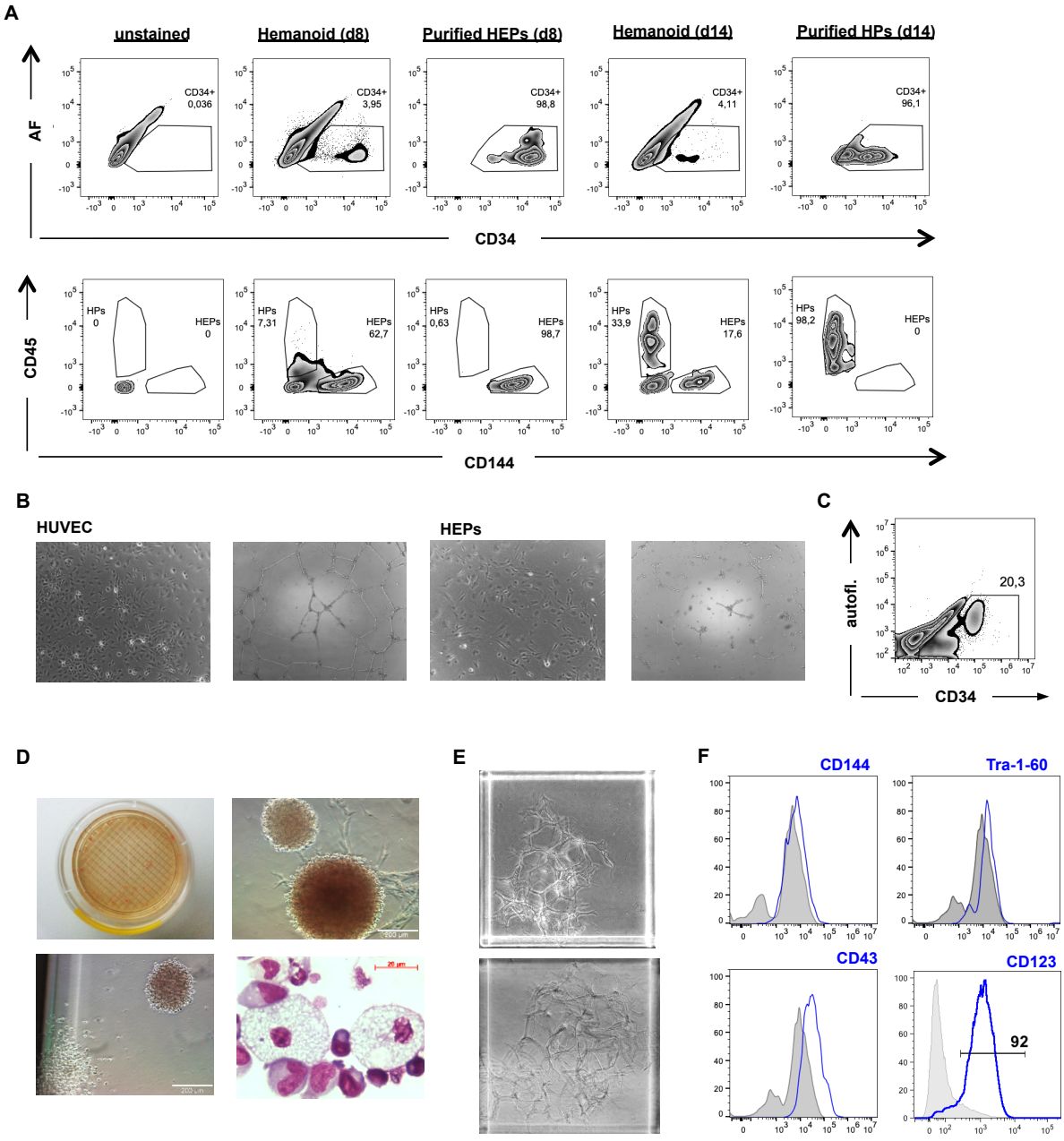

Supplementary Figure 3. Characterization of hemato-endothelial progenitors (HEPs) and hematopoietic progenitors (HP) within the hemanoids. (A) FACS strategy for purification of HEPs and HPs. Pre-gating on total $CD34^+$ cells (upper panel) was followed by separation between $CD34^+/CD144^+$ HEPs and $CD34^+/CD45^+$ HP (lower panel). Re-analysis of sorted HEPs and HPs shows high purification efficacy (middle and right panel, percentage of gated population is indicated). **(B)** Morphology of HUVECs and HEPs at day 6 post sorting and culture in endothelial (EBM2) medium (10x magnification, left pictures) and tube formation by HUVECs and HEPs in semisolid medium (3 days post sorting, 15.000 cells/12 well, picture taken after 29 hours). **(C)** Flow cytometry analysis of HEP cells after 1 week EHT culture. After FSC/SSC gating on the viable cell population, pre-gating on $CD34^+$ was used to identify human HEP-derived cells and exclude murine OP9 stromal cells (percentage of gated population is indicated). **(D)** Colony forming units (CFU) of HEP-derived cells after EHT culture when cultured in methylcellulose (scale bars: 100µm and 200µm, respectively) and representative cytospin staining of CFUs flushed out of the methylcellulose (scale bar: 20µm). **(E)** HEPs seeded in methylcellulose. **(F)** Flow cytometry analysis of HPs presented as histogram overlay: unstained grey filled, surface marker expression blue (percentage of gated population is indicated).

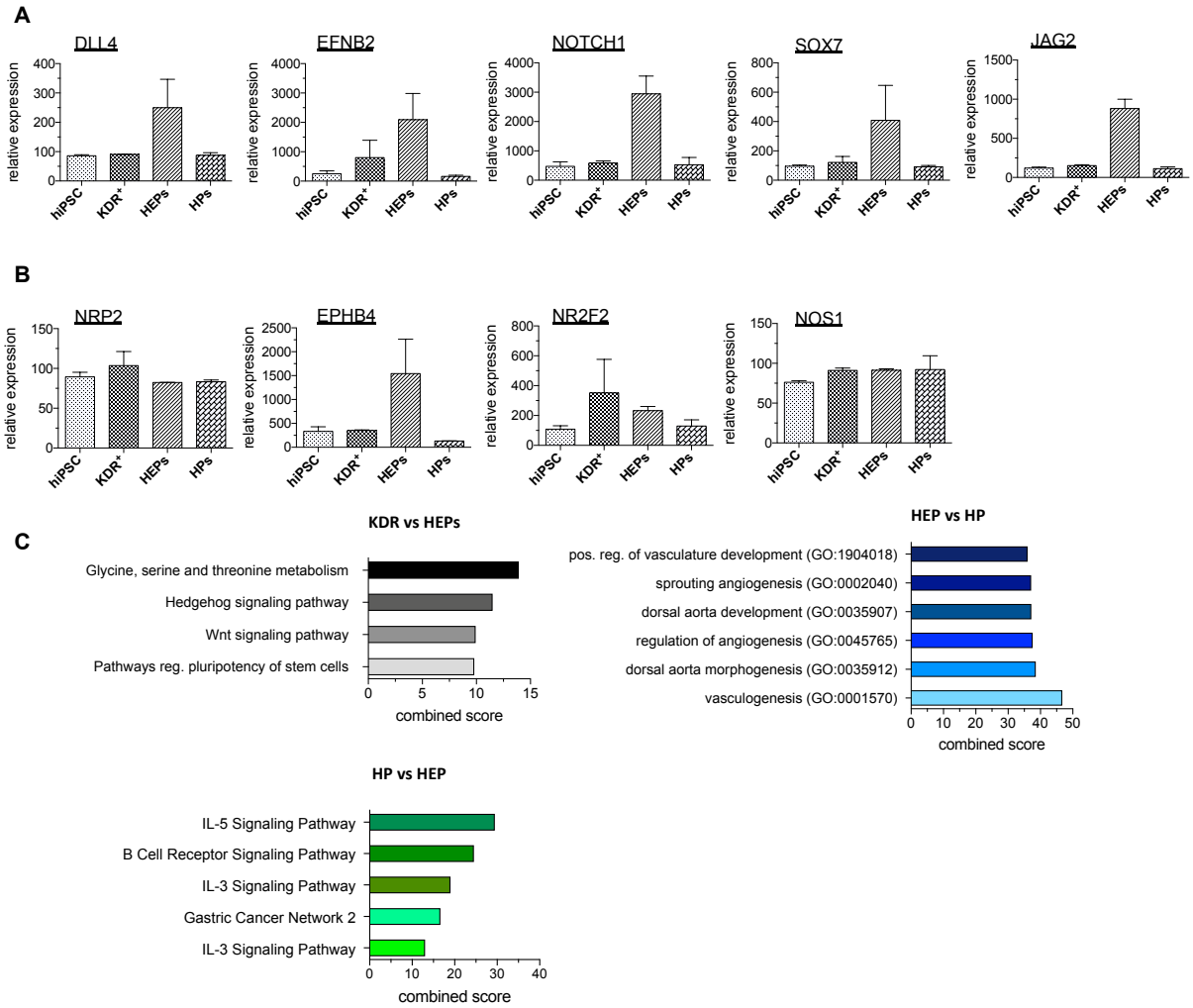

Supplementary Figure 4: Whole transcriptome analysis of defined populations during hematopoietic specification. FACS purified TRA-1-60^{+} pluripotent iPSC, TRA-1-60^{-}/KDR^{+} mesodermal progenitor cells derived from EBs, CD34^{+}CD144^{+}CD45^{-} HEPs and CD34^{+}CD144^{-}CD45^{+} HPs derived from the hemanoids were analysed by microarray analysis. **(A)** Arterial and **(B)** venous genes analysed in different populations (relative expression, n=2, mean±SD). **(C)** Pathway analysis of top 100 upregulated genes in KDR^{+} mesoderm compared to iPSC (upper left, KEGG pathways), HEPs compared to HPs (upper right, GO Biological Processes) and HPs compared to HEPs (lower panel, WikiPathways) using EnrichR.

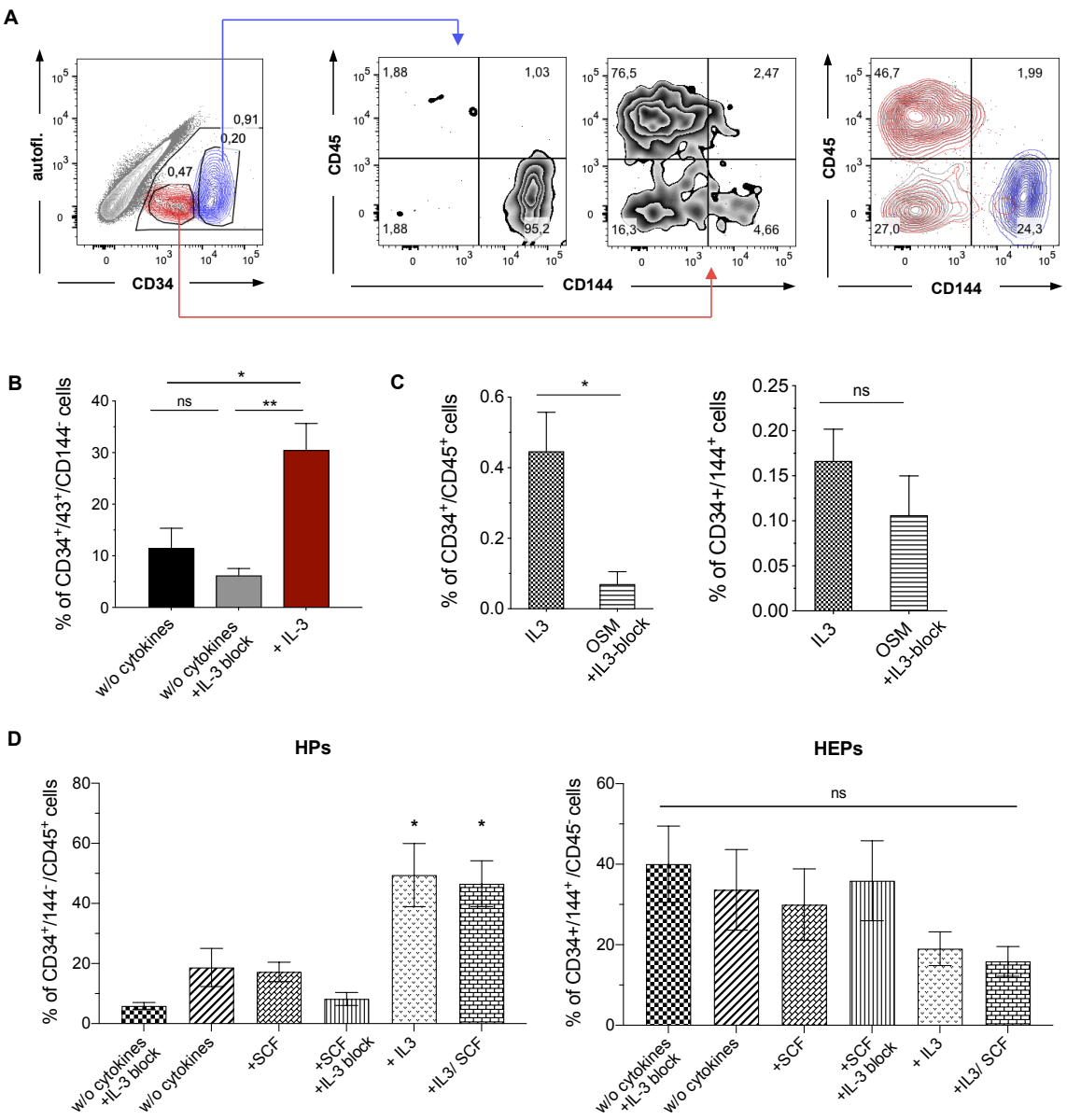

Supplementary Figure 5. Influence of IL-3 on the EHT of HEPs. **(A)** Left: CD34 expression in dissociated hemanoids_d8 cultured in medium with IL-3 supplementation clearly shows two separate populations: $CD34^{high}$ cells (depicted in blue) and $CD34^{low}$ cells (depicted in red, left plot). Middle: When further analyzing the fate of this cells, $CD34^{high}$ cells represent $CD144^{+}/CD45^{-}$ HEPs whereas the majority of $CD34^{low}$ cells represents $CD144^{-}/CD45^{+}$ HPs. Right: Overlay of $CD34^{high}$ (blue) and $CD34^{low}$ (red) populations with respect to CD45 and CD144 expression (percentage of gated population is indicated). **(B)** Frequency of $CD34^{+}43^{+}144^{-}$ cells in hemanoids cultured without (w/o) cytokines, (w/o) cytokines +IL-3 blocking antibody (+IL-3 block) or in presence of IL-3 on day 16 of differentiation (n=5, mean±SEM). **(C)** Flow cytometry analysis of $CD34^{+}/CD144^{+}$ HEPs and $CD34^{+}/CD45^{+}$ HPs in hemanoids cultured with IL-3 or OSM+IL-3blocking AB in hemanoids at d16 of differentiation (n=3, mean±SEM). **(D)** Analysis of $CD144^{+}/CD45^{-}$ HEPs and $CD144^{-}/CD45^{+}$ HPs among total $CD34^{+}$ cells within hemanoids cultured w/o cytokines +IL-3 blocking antibody, w/o cytokines, with SCF, SCF +IL-3 blocking antibody, with IL-3 and with a combination of IL-3 + SCF (n=3, mean±SEM).

(*p<0.05, ns denotes not significant; statistical significances were assed using One-way ANOVA with Tukey's multiple comparison test).

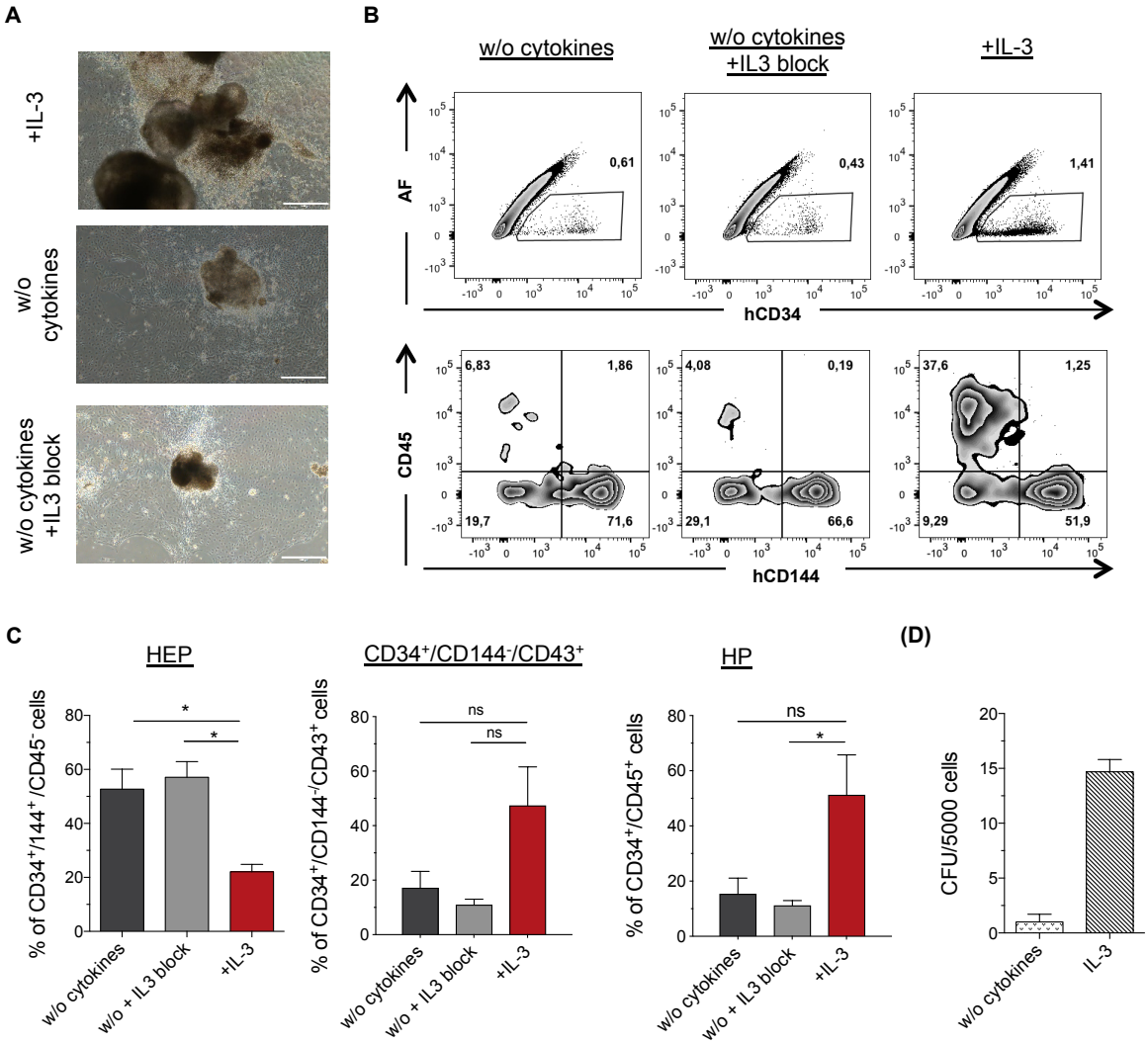

Supplementary Figure 6: Influence of IL-3 on the EHT of HEPs derived from F134iPSC. (A) Representative light microscopy of F134iPSC-derived hemanoids cultures cultured in the presence of IL-3, without (w/o) cytokines, or w/o cytokines+IL-3 blocking antibody (IL-3 block, scale bar: 500um). **(B)** Analysis of total $CD34^+$ cells (upper row) and HEPs and HPs among total $CD34^+$ cells (lower row) within the F134iPSC-derived hemanoids on day 16 of differentiation (percentage of gated population is indicated) and **(C)** quantification of n=3, mean±SEM. **(D)** CFUs in methyl-cellulose after EHT culture on OP9 stromal cells in the presence or absence of IL-3 (n=2, technical replicates, mean±SD). (*p<0.05, **p<0.01, ***p<0.001, ****<0.0001, ns denotes not significant; statistical significances were assed using One-way ANOVA with Tukey's multiple comparison test).

Supplementary Material&Methods:

Generation of the CD144.GFP hIPS-reporter-line:

A 2.5 kb subfragment of the CD144 promoter (kindly provided by Phillip Huber, Department of Cellular Responses and Dynamics, CEA-INSERM-Joseph Fourier University, France, [1]) was incorporated into a lentiviral vector harboring an eGFP reporter gene. To prevent epigenetic silencing, the promoter was inserted after a CBX3 minimal ubiquitous chromatin opening element (UCOE) [2]. Human iPSC were transduced with the lentiviral vector CBX3.CD144.eGFP with a multiplicity of infection (MOI) of 10 as single cells in a matrigel-based, feeder free culture as described in [3].

RNA isolation and qRT-PCT:

RNA was isolated with Phenol/Chloroform. mRNA was reverse transcribed using the First strand cDNA synthesis kit (Thermo Fischer Scientific) following the manufactures instructions. Quantitative RT-PCR was performed using a on a StepOnePlus light cycler (Applied Biosystems). The following pre-designed SYBRgreen assays were obtained from Quantitect Primer Assays (Qiagen): HS_MIXL (QT00211561), HS_KDR1 (QT00069818), HS_GATA2 (QT00045381), HS_TAL1 (QT00012530), HS_GAPDH (QT QT00079247).

For microarray analysis RNA was isolated using the RNA Kit (Quiagen).

Clonogenic Assay:

Different cell types were seeded in methylcellulose medium (HSC003, R&D Systems or MethoCult™ H4435 Enriched Stem Cell Technologies) and allowed to grow for 14 days before colonies containing more than 50 cells were counted.

Endothelial Culture:

CD144-positive sorted cells from dissociated hemanoids were cultures in EBM (Endothelial Cell Growth Basal Medium) 2 (Lonza) and passages using incubation with Trypsin for 3 min.

Tube Formation:

15.000 HEPs or HUVECs were cultured in semi-solid Matrigel. Brightfield microscopy was performed 27 hours after seeding.

Cytospins:

Cytospins were generated utilizing a shandon cytocentrifuge (Thermo Scientific, Waltham, MA, USA). Slides were stained for 5 min in May-Grünwald stain and 10 min in 5% of Giemsa Azur-Eosin-Methylenblue solution and washed extensively in aqua dest.

RNA *in situ* hybridization analyses:

Whole-mount *in situ* hybridization followed a standard procedure with digoxigenin-labeled antisense riboprobes [4]. Stained specimens were transferred in 80% glycerol prior to documentation. *In situ* hybridization on 10-µm paraffin sections was performed as described[5]. For each marker, at least three independent specimens were analysed.

Flow Cytometry:

In order to perform flow cytometry analysis, iPSC, EBs or hemanoids were dissociated to single cells by incubation with TrypLE (Thermo Fischer Scientific) for 10-40 min at 37°C. Intermediate pipetting was performed to accelerate the dissociation process. PBS supplemented with 2 mM EDTA and 5% FCS (FACS buffer) was used during the staining process. Cells were rinsed with FACS buffer and analysed with a FACS Calibur (BD), LSR (BD) or cytoflex (Beckman Coulter) machine. Raw data was analysed using FlowJo software (TreeStar, Ashland, OR). Single stained samples were used to setup compensation for multicolor stainings.

Used antibodies were:

Antigen	Fluorochrome	Catalognumber	Provider
CD45	PE	304008	Biolegend
CD11b	APC	17-0118	eBioscience
CD14	PE	12-0149	eBioscience
CD163	APC	17-1639	eBioscience
CD34	FITC	11-0349	eBioscience
CD66b	APC	17-0666	eBioscience
CD16	FITC	302005	Biolegend
TRA-1-60 (Podocalyxin)	PE	330609	Biolegend
CD144	APC	17-1449	eBioscience
CD43	PE	560199	BD Bioscience
CD45	PE-Cy7	25-0459	eBioscience
CD309/KDR	PE-Cy7	359911	Biolegend
CD309/KDR	AF647	338909	Biolegend
CD235a	PerCp-Cy5.5	349109	Biolegend
CD235a	PE	12-9987	eBioscience

Immunofluorescent staining:

Cells were fixed with 4% paraformaldehyde (w/v) and stained by standard protocols using primary antibodies anti-beta3-Tubulin (Upstate, NY, USA(05-559); IgG2a, 1:400), anti-AFP (R&D Systems, Minneapolis, USA(189502); IgG1, 1:800) and anti-Desmin (Progen, Heidelberg, Germany(10519); IgG1, 1:20) and secondary antibody DyLightÒ549-donkey-anti-mouse-IgG (1:200, Jackson Immunoresearch Laboratories (715-165-150). Corresponding isotype antibodies were used for negative control staining. Cells were counterstained with DAPI (Sigma).

Histology and immunohistochemistry:

For histologic and immunohistologic stainings embryoid bodies and hemanoids were fixed o/n at 4°C, stored in PBS until dehydration in a graded ethanol series and subsequently embedded in paraffin. Paraffinised samples were sliced into 3 µm sections with an RM 2265 microtome (Leica), rehydrated and stained with H&E for histologic analyses.

Prior to immunohistochemical analyses sections were rehydrated and underwent antigen retrieval (Dako). The samples were then blocked in 1% BSA in PBS and incubated with anti-CD45 (Stem Cell, 60018) 1:100 in blocking solution. Detection of the primary antibody was achieved by incubation with peroxidase conjugated goat anti mouse IgG1 (Jackson, 115-035-205) 1:500 in blocking solution and subsequent staining with DAB+ substrate (Agilent, K346711-2). Counterstaining of nuclei was performed with hematoxylin.

Selected marker proteins of differentiation were analyzed via immunohistochemistry. Briefly, antibodies were used as follows: anti-vimentin (1:100 from (DAKO, M0725), anti-CD68 (1:100 from DAKO, M0876)), anti-CD56 (1:100 from DCS, C1596C01)), anti-smooth muscle actin (1:100 from DAK, M0851) and anti-pan-Cytokeratin (1:200 from DAKO, M3515). All antibodies were visualized using the (DAB detection kit, Roche).

Statistics:

GraphPad Prism 7 or 8 was applied to perform unpaired Student's T test or analysis of variance (ANOVA). Asterisks mean: * P< .05; ** P< .01; ***P< .001

Supplementary References:

1. Prandini MH, Dreher I, Bouillot S, Benkerri S, Moll T, Huber P. The human VE-cadherin promoter is subjected to organ-specific regulation and is activated in tumour angiogenesis. Oncogene. 2005;24(18):2992-3001.
2. Muller-Kuller U, Ackermann M, Kolodziej S, et al. A minimal ubiquitous chromatin opening element (UCOE) effectively prevents silencing of juxtaposed heterologous promoters by epigenetic remodeling in multipotent and pluripotent stem cells. Nucleic Acids Res. 2015;43(3):1577-1592.
3. Lachmann N, Happle C, Ackermann M, et al. Gene correction of human induced pluripotent stem cells repairs the cellular phenotype in pulmonary alveolar proteinosis. Am J Respir Crit Care Med. 2015;189(2):167-182.
4. Wilkinson DG, Nieto MA. Detection of messenger RNA by in situ hybridization to tissue sections and whole mounts. Methods Enzymol. 1993;225(361-373.
5. Moorman AF, Houweling AC, de Boer PA, Christoffels VM. Sensitive nonradioactive detection of mRNA in tissue sections: novel application of the whole-mount in situ hybridization protocol. J Histochem Cytochem. 2001;49(1):1-8.